Experimental and numerical study on lateral and longitudinal resistance of ballasted track with nailed sleeper

Guo, Yunlong; Zong, Lu; Markine, Valeri; Wang, Xinyu; Jing, Guoqing

DOI
10.1080/23248378.2021.1872424

Publication date
2021

Document Version
Accepted author manuscript

Published in
International Journal of Rail Transportation

Experimental and numerical study on lateral and longitudinal resistance of ballasted track with nailed sleeper

Yunlong Guo[1], Lu Zong[2], Valeri Markine[1], Xinyu Wang[2], Guoqing Jing[2] *

1. Faculty of Civil Engineering and Geosciences, Delft University of Technology, Delft, 2628CN, Netherlands
2. School of Civil Engineering, Beijing Jiaotong University, Beijing, 100044, China
*. Corresponding author
Email addresses: gqjing@bjtu.edu.cn (G. Jing)

Abstract: Lateral and longitudinal resistance of ballasted track are two main indicators for the track stability quantification. Aiming at improving the lateral and longitudinal resistance, an innovated sleeper (nailed sleeper) is studied with single sleeper push tests (SSPTs) and discrete element modelling (DEM). The SSPTs were applied to study how much resistance the nailed sleeper can improve, considering different nail lengths (100, 200, 400 mm), and also used to calibrate and validate the DEM models. Afterwards, with the validated DEM models, different simulation conditions were performed and compared to confirm the optimal nail sleeper, including nail length (100, 200 mm) and nail number (2, 4). Results show that applying nailed sleepers improves the lateral resistance by 53.7% and the longitudinal resistance by 39.2%. The numerical results show that 4 nails, compared to 2 nails, can increase lateral and longitudinal resistance by 20.2% and 10.6% (nail length: 100 mm) as well as 37.0% and 33.5% (nail length: 200 mm), respectively. This study is helpful for the railway ballasted track construction and design in some special areas that need sufficient lateral and longitudinal resistance, e.g. mountainous area, bridge and tunnel.

Keywords: longitudinal resistance; lateral resistance; track stability; DEM; nailed sleeper; ballasted track

1. Introduction

In recent decades, considerable studies have been performed on the continuously welded rail (CWR) track concerning the safety and performance, which is due to the growing CWR tracks are applied for replacing the jointed tracks (Zhai, 2020). The main purposes of the replacement are Improving the ride quality, increasing the service life of the rail and vehicle, as well as reducing the maintenance cost (Bakhtiary, Zakeri and Mohammadzadeh, 2020). Nevertheless, after removing the joints, the possibility of the undesirable derailments increases because of the track buckling (summer) and the rail fracture (winter) (Kish and Samavedam, 2013). Both of them are related to the loss of track stability (Indraratna and Ngo, 2018).

For the track stability, the ballast layer is the most important track component, and sufficient sleeper resistance from ballast layer are the guarantee for the track stability and ride comfort (Jing and Aela, 2019, Guo, Markine, Zhang, Qiang and Jing, 2019). Particularly, ballast layer provides the lateral resistance in the range of 50%-70% among rail (10%), fastening system (30%) and ballast layer (60%) (Jing and Aela, 2019). The three types of resistance provided by the ballast layer are the lateral resistance, longitudinal resistance and vertical support to sleepers. According to the Chinese design code for high speed and heavy haul railways (China, 2014), the three types of resistance should meet the requirements in Table 1.

Table 1 Requirement for the ballast layer resistance per sleeper

Operating speed (km/h)	Longitudinal resistance (kN)	Lateral resistance (kN)	Vertical stiffness (kN/mm)
200~250	≥12	≥10	≥110
250~300	≥14	≥12	≥120

Even though the ballasted track is constructed according to the standards, the track stability guarantee still remains a challenge due to the following aspects. Firstly, the operation of higher speed and heavier haul trains leads to the higher frequency and larger amplitude loadings, respectively, which accelerate the ballast degradation and track geometry irregularity (Zhang, Zhao, Zhai, Shi and Feng, 2018). Secondly, the ballast

layer profile is reduced to avoid the ballast flight phenomenon in the high speed railway, for example, the ballast shoulder height is reduced to 0 cm (Jing, Ding and Liu, 2019). This may lead to track instability. Lastly, some special areas have some difficult engineering conditions and issues, e.g. the high speed line in the cold region (Moscow-Kazan) and high speed line in earthquake region (Tehran-Isfahan). Particularly, the passenger and freight railway line from Sichuan to Tibet is in the mountainous region, which is built with the maximum operation speed at 200 km/h and the maximum axle load at 25 ton. The maximum length of the slope can be over 60 km and the steepest slope can reach the gradient 3%. The longitudinal resistance is usually not sufficient at the long and steep slopes, which will further lead to the differential settlement and hanging sleeper (Jing and Aela, 2019).

To guarantee the track stability, countermeasures are proposed and studied in three aspects. Firstly, the ballast layer is enhanced with the application of new materials. The new materials include the geogrid (Qian, Mishra, Tutumluer and Kazmee, 2015), polyurethane (Gundavaram and Hussaini, 2019), geocell (Kaewunruen, Remennikov and Aikawa, 2016), steel slag (Qi, Indraratna, Heitor and Vinod, 2018), tyre-derived aggregates (Fathali, Nejad and Esmaeili, 2017), Neoballast (Sol-Sánchez, Moreno-Navarro, Rubio-Gámez, Manzo and Fontseré, 2018), under sleeper pads (Navaratnarajah, Indraratna and Ngo, 2018) and under ballast pads (Lima, Dersch, Qian, Tutumluer and Edwards, 2018). The studies have proved that applying new materials to ballast layer can increase the ballasted track stability and performance. For example, using the geogrid and geocell increases 42% lateral resistance and reduce 122% ballast permanent settlement (Indraratna, Hussaini and Vinod, 2013). Using the ballast glue increases minimum 31% lateral resistance (Jing, Zhang and Jia, 2019). Rail support modulus is increased to 1.64 times and lateral resistance is increased by 27% when applying steel slags as ballast (Esmaeili, Nouri and Yousefian, 2016). Nevertheless, the concerns of new material application are 1) material costs, 2) installation problem and 3) maintenance consideration (tamping).

Additionally, enhancing the interaction between the ballast layer and the sleeper is used to improve track stability. For example, the profile size of ballast layer, including shoulder height, shoulder height and slope, is increased in (Powrie and Le Pen, 2011) to study the lateral resistance increment. Another example is applying the sleeper anchor to the sleeper (Jing, Ji and Aela, 2020). However, Increasing the ballast layer profile can increase the ballast flight possibility, and to date, the sleeper anchor has only been utilised for the wooden sleeper.

Lastly, the innovated types of sleepers are developed and studied, e.g. Y-shape sleeper, ladder sleeper, steel sleeper, frictional sleeper and winged-shape sleeper (Jing and Aela, 2019, Koike, Nakamura, Hayano and Momoya, 2014). The new types of sleepers are focusing on the sleeper material and shape, and they are able to provide higher lateral resistance from the earlier study results. To be more specific, 50% lateral resistance is increased by the winged-shape sleeper. The peak lateral resistance of ladder sleeper can reach 15 kN/m, which increases 55% than normal sleepers. 63-70% lateral resistance is increased by frictional sleepers. Particularly, the nailed sleeper was proposed in (Esmaeili, Khodaverdian, Neyestanaki and Nazari, 2016) that increases 200% lateral resistance.

From the above-mentioned studies, three aspects can be stressed. Firstly, most of the studies focus on the vertical stiffness and lateral resistance of the ballast layer, and limited studies are performed on the longitudinal resistance (Liu, Xiao, Wang, Liu, Gao and Li, 2018). The limited studies cannot always draw the same conclusions, consequently, more studies should be performed. To be more specific, the lateral and longitudinal resistance of the in the field are measured in [46], and the single sleeper push test model is built. The influences of shoulder ballast (slope, width, height), particle size distribution (PSD) on the lateral and longitudinal resistance are studied in (Zeng, Song, Wang, Yan, Wang and Xiao, 2018). In (Mohammadzadeh, Esmaeili and Khatibi, 2018), the longitudinal resistance to the track panels is measured, interestingly, the results of longitudinal stiffness per sleeper are with difference by two times. In (Liu, Xiao, Wang, Liu, Gao and Li, 2018), cyclic longitudinal loadings are applied to the track panel, and the resistance-displacement hysteretic curves are analysed. These studies only measured the longitudinal resistance, and did not provide a solution for improving the longitudinal resistance.

Secondly, it can be observed that innovated sleepers can improve lateral resistance, and among them the nailed sleeper is the optimal one with the following advantages. 1) it can increase 200% lateral resistance, which is the highest among all the sleepers (Esmaeili, Khodaverdian, Neyestanaki and Nazari, 2016). 2) the nailed sleeper does not affect the maintenance process (e.g. tamping). 3) the nailed sleeper can provide longitudinal resistance and higher vertical stiffness. However, how much longitudinal resistance of the nail sleeper can increase has not been studied, and in (Esmaeili, Khodaverdian, Neyestanaki and Nazari, 2016)

the nail was stabbed into the subgrade, which may cause the subgrade instability due to the rainfall. Therefore, shorter nail that is stabbed only into ballast layer (or to the sub-ballast layer) needs to be studied on how much stability can be increased.

Lastly, most of the studies apply the field tests or experimental tests (Liu, Xiao, Wang, Liu, Gao and Li, 2018, Mohammadzadeh, Esmaeili and Khatibi, 2018, Esmaeili, Zakeri and Babaei, 2017, Le Pen, Bhandari and Powrie, 2014, De Iorio, Grasso, Penta, Pucillo, Rossi and Testa, 2016), and limited studies have been performed with a combination of discrete element method (DEM) simulations and experimental tests (Khatibi, Esmaeili and Mohammadzadeh, 2017). Combining the DEM simulation and experimental tests can control the test configurations and conditions more easily (Xiao, Zhang, Wei and Luo, 2017). In addition, it has been demonstrated the application feasibility of the DEM to study the track stability (Guo, Zhao, Markine, Shi, Jing and Zhai, 2020). The DEM is a powerful tool for granular material studies. It can reflect the mechanism of the track stability from particle level (i.e. mesoscopic level) (Guo, Zhao, Markine, Jing and Zhai, 2020). To be more specific, the DEM is able to 1) acquire all the particle information, such as velocity, displacement, rotation, acceleration, contact force etc., 2) consider the ballast physical properties, e.g., density, size, shape etc. and 3) simulate the ballast degradation, e.g., particle breakage and abrasion (Xiao, Zhang, Wei and Luo, 2017).

Consequently, towards these research gaps, the combination of experimental tests and DEM simulations are performed to study how much track stability the nailed sleeper can increase. Moreover, how much resistance can be increased by the nails is also studied. The experimental tests include the lateral SSPTs and the longitudinal SSPTs to measure the lateral and longitudinal resistance of the nailed sleeper and normal sleeper. Note that to date no studies were found on longitudinal resistance measurement of nailed sleeper. The two tests are confirmed to be effective and they are widely-used in many studies (Esmaeili, Khodaverdian, Neyestanaki and Nazari, 2016, Zeng, Song, Wang, Yan, Wang and Xiao, 2018, Esmaeili, Zakeri and Babaei, 2017). According to the configurations of the two tests, the corresponding DEM models were built (SSPT model) with the DEM with the consideration of nail lengths (100 or 200 mm) and number (2 or 4). The simulation results and test results were compared, and the models were validated. Afterwards, the track stability mechanism of the nailed sleeper from particle level was presented, from the viewpoint of contact force (between sleeper and ballast). Further, the optimal depth of the nailed sleeper is confirmed based on the lateral and longitudinal resistance results. This is helpful for applying the nailed sleeper for a railway line in some special areas, e.g. the long and steep slope railway line.

2. Methodology

2.1. Experimental test

2.1.1. Test materials

The ballast track dimensions to perform the SSPT, as well as the ballast properties can be found in (Guo, Fu, Qian, Markine and Jing, 2020). The particle size distribution (PSD) is given in Figure 4(c), which meets the British standard (British Standards Institution, 2013). Two types of sleepers were applied in the SSPTs. One was the Chinese mono-block sleeper, which is the most common type applied in Chinese railway. The other was the nailed sleeper, which is built based on mono-block sleeper with two holes, as shown in Figure 1. The two holes are used for inserting nails with the diameter at 40 mm, and the nails of different lengths were applied but they were with the same diameter at 35 mm.

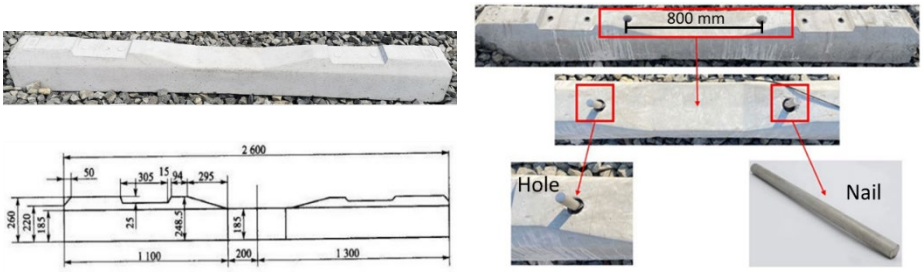

Figure 1 Chinese mono-block sleeper (left) and nailed sleeper (right)

2.1.2. Test setup

The facilities applied for the SSPTs include the hydraulic jack, dial indicator, pressure sensor and data acquisition system. The maximum loading of hydraulic jack is 20 ton, which is sufficient to provide enough force to move the sleeper until the peak resistance value. The actuator stroke can travel at most 10 cm. The travelling distance is enough for reaching the required maximum sleeper displacement. The dial indicator precision is 0.001 mm, and can measure distances at most 30 mm. The pressure sensor can measure the loading in the range of 0~15 ton, and the data acquisition system is used to collect the force data from pressure sensor.

Lateral single sleeper push test

The setup of the lateral SSPT is shown in Figure 2a. Normally, the lateral SSPT is a common laboratory means to measure the lateral resistance of ballast layer to the sleeper. During the SSPT, the sleeper is moved by the force-applying devices (hydraulic jack), meanwhile the applied forces and the corresponding sleeper displacement are measured with the pressure sensor and the dial indicator, respectively. The sleeper displacement is recorded with the maximum value at around 5 mm in normal conditions.

Specifically, before moving the sleeper the four sleeper fasteners were removed, afterwards, the hydraulic jack was installed between the sleeper and a device that provide enough resistance, as shown in Figure 2a. In other words, the sleeper was pushed by the hydraulic jack against the resistance-providing device. The loading interval was 30 seconds between force-applying steps. The pressure sensor was installed together with the hydraulic jack actuator, and it was connected to the computer system recording the loading forces. The two dial indicators were placed on the other side of the sleeper for measuring the sleeper displacement, and the average value was used as the lateral sleeper displacement.

Longitudinal single sleeper push test

Figure 2b presents the of the LSSPT setup. The hydraulic jack actuator and the pressure sensor were placed between two adjacent sleepers. One of the two sleepers was fixed to provide enough resistance, and the other sleeper was pushed by the step-loading (intervals 20 seconds). The pressure sensor was put in the middle of jack actuator and measured sleeper, and it was connected to the data acquisition system. Two dial indicators were placed at the other side of the pushed sleeper to measure the longitudinal displacement of the sleeper, and the average value was used as the longitudinal sleeper displacement.

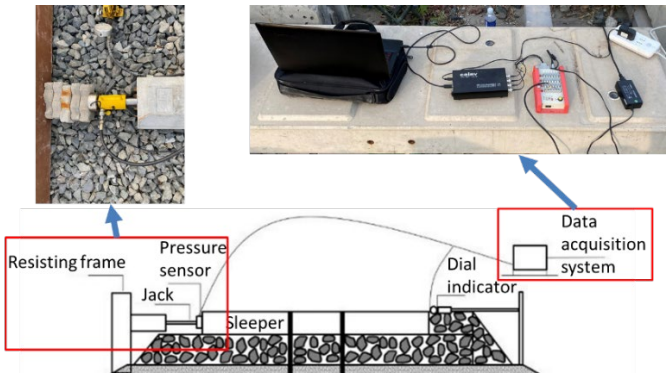

(a)

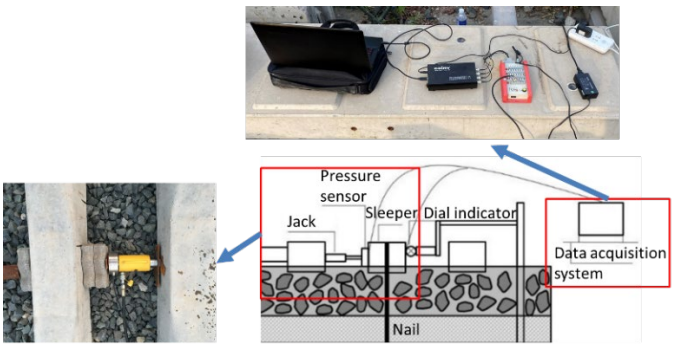

(b)

Figure 2 Single sleeper push test and longitudinal single sleeper push test setup (a) Lateral single sleeper push test (b) Longitudinal single sleeper test

2.1.3. Test conditions

The main purpose of the study is confirming 1) how much the nailed sleeper can increase the lateral and longitudinal resistance, 2) how much the nail length and number influence the resistance and 3) how much the nails can increase the resistance. Because in the high speed railway the ballast layer profile is reduce, e.g. the flat should height and reduced shoulder width. Moreover, in some special areas, e.g. mountainous area with long steep slope, the longitudinal resistance is in most cases not sufficient. Most importantly, the contributions of ballast bed, crib and shoulder forces to the longitudinal resistance were also presented by the tests.

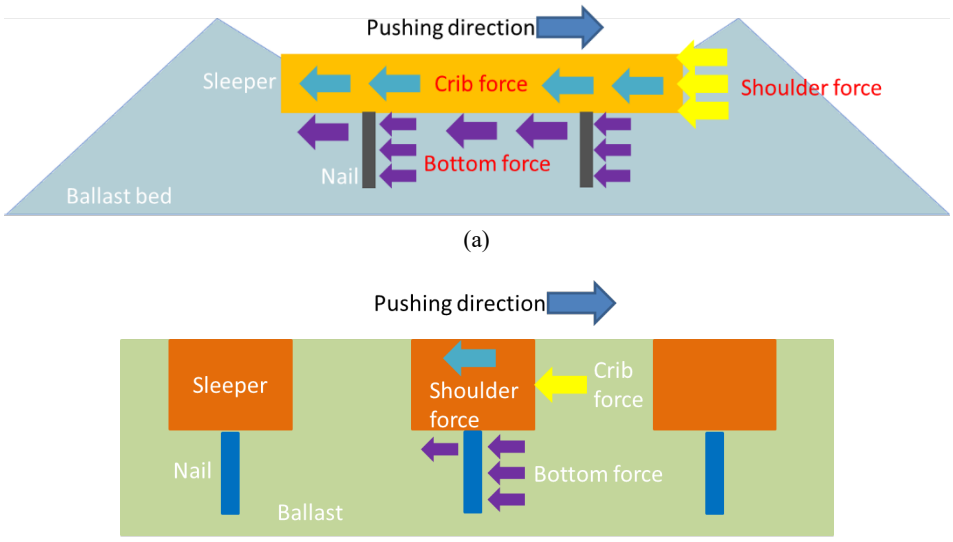

Figure 3 Contribution of three ballast layer parts to lateral or longitudinal resistance (a) Lateral resistance contribution of three parts (b) Longitudinal resistance contribution of three parts

Consequently, the test conditions are designed as the nailed sleeper (with different nail length) combined with the different ballast layer profile (shoulder height and width), as shown in Table 2. While nail number influences on resistance were studied with DEM models. Moreover, the nail increment to the resistance can be presented by the contribution of three ballast layer parts to the resistance, as shown in Figure 3. The three parts include ballast bed, crib ballast and shoulder ballast. The ballast bed contribution (lateral and longitudinal resistance) was measured and the ratio of it to the total resistance was used to present the nail increment to the resistance. The ballast bed contribution was measured by removing the crib ballast and shoulder ballast, afterwards, the sleepers were pushed laterally or longitudinally as the same procedure of the normal lateral and longitudinal SSPTs.

Table 2 Configurations and conditions of lateral and longitudinal single sleeper push tests

Condition	Test name	Sleeper type	Nail length (mm)	Shoulder width (mm)
A	Lateral SSPT	Mono-block	-	500
B	Lateral SSPT	Nailed sleeper	400	500
C	Lateral SSPT	Nailed sleeper	200	500
D	Lateral SSPT	Nailed sleeper	100	500
E	Lateral SSPT	Nailed sleeper	400	400
F	Lateral SSPT	Nailed sleeper	400	300
G	Longitudinal SSPT	Mono-block	-	500
H	Longitudinal SSPT	Nailed sleeper	400	500
I	Longitudinal SSPT	Nailed sleeper	200	500
J	Longitudinal SSPT	Nailed sleeper	100	500
K	Longitudinal SSPT	Nailed sleeper	400	400
L	Longitudinal SSPT	Nailed sleeper	400	300

2.2. Numerical simulation

As shown in Figure 4, the lateral and longitudinal SSPT models are presented with the DEM. In the DEM models, the Sphere and Wall are basic elements. The SSPT models consisted of ballast layer and two sleepers, which were based on the test configurations.

2.2.1. Ballast layer and sleepers

To be more specific, the ballast particles in the models were modelled with spheres, and they were generated with different sizes fitting the particle size distribution, as shown in Figure 4b. Five sleeper models were built using the AutoCAD. The sleeper models were exported in the DEM models, as shown in Figure 4c.

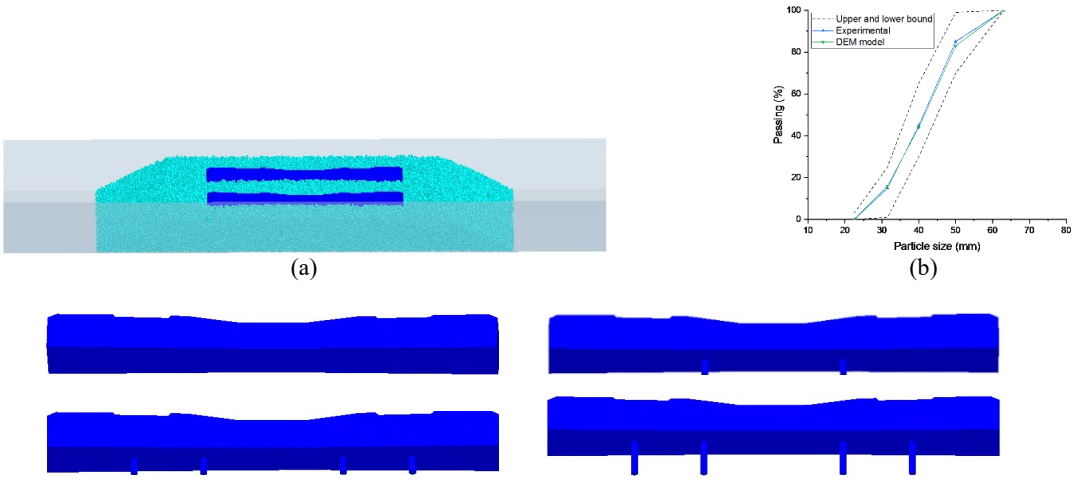

Figure 4 Single sleeper push test and longitudinal single sleeper push test models (a) single sleeper push test model overview (b) Particle size distribution (c) Mono-block sleeper and nailed sleeper

Most ballast-related studies using the DEM built ballast particles as clump or cluster, which are sphere assemblies to present one ballast particle. They can consider the ballast shapes and particle breakage. However, it takes huge amounts of computational costs, which means the clump or cluster cannot be applied in big models, e.g. full scale track model. In the SSPTs ballast breakage is impossible to occur due to slow and low magnitude loading, therefore, simple spheres were used in the SSPT models to simulate ballast particles. It needs to note that the ballast shape can also be compensated by adding rolling friction when applying the spheres as ballast particles, which has been proved in (Irazábal, Salazar and Oñate, 2017).

It needs to note that the Application Program Interface (API) was applied for making the modelled sleepers to have weight. In other words, the API was applied to slightly make the sleeper (walls) move until the reaction force reaches the weight. It is similar to the servo control that explained in (Suiker and Fleck, 2004).

2.2.2. Model Parameters

The parameters used in the models are given in Table 3. Before building the elements, the material properties (bulk and equipment materials) should be defined. In the SSPT models, the spheres (ballast particles) were the bulk material, while the track components built by walls (sleeper and boundary) were equipment material. The default contact model, Hertz-Mindlin contact model is applied in the SSPT models. The contact model is used to do the calculation of the contact forces between two elements, including wall-sphere and sphere-sphere. The contact force value is primarily calculated by the parameters of the material properties (Guo, Zhao, Markine, Jing and Zhai, 2020).

Table 3 Parameters for lateral and longitudinal single sleeper push test models

Parameters	Ballast (spheres)	Sleeper (walls)
Density (10^3 kg/m^3)	2.7	2.5
Poisson ratio	0.2	0.2
Young's modulus (GPa)	24	2.4
Coefficient of restitution	0.5	0.5

Coefficient of static friction	1.5	2.0
Coefficient of rolling friction	2.0	1.8

Ballast materials have different material properties, and they were mostly presented in the earlier studies, which means the values of the parameters can be directly applied in the SSPT models, e.g. density. However, several ballast material properties are not able to apply in SSPT models. These properties need some modifications, because the contacts in the DEM are simplified compared with the real contacts. For instance, Young's modulus of ballast materials can be approximately 30 GPa (Esveld and Esveld, 2001). However, in earlier studies, Young's modulus in DEM models is always set as a lower value. This is due to the contact area in reality is much lower than in the DEM. Therefore, the Young's modulus was set as 24 GPa in this study. Several ballast properties are confirmed through the laboratory tests, such as direct shear test, triaxial test and confined compression test. The properties include the coefficient of restitution, coefficient of static friction and coefficient of rolling friction .

As shown in Table 4, it presents the values of ballast properties that were used in the DEM models. From the table, it can be seen that the values are within the range and can be used for further study with different test conditions. While the coefficient of restitution, coefficient of static friction and coefficient of rolling friction were obtained by comparing the simulation results with the experimental results.

Table 4 Parameters in DEM models used in earlier studies

Parameters	Values in earlier studies (Guo, Zhao, Markine, Jing and Zhai, 2020)
Density (10^3 kg/m^3)	2.5 to 2.7
Poisson ratio	0.18 to 0.2
Young's modulus (GPa)	2.4 to 24

2.2.3. SSPT model creation procedure

As shown in Figure 5, the model creation procedure is presented. After sphere properties and wall properties were defined, a container that was a certain size geometry was built for filling in ballast particles (spheres).

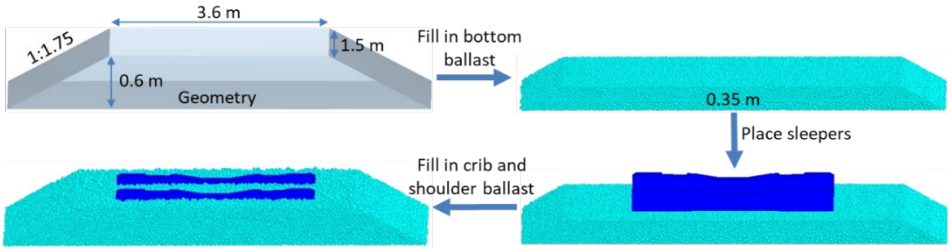

Figure 5 Creation method of the test models

Firstly, the geometry was built according to the SSPTs with the upper base at 3.6 m, slope at 1:1.75 and height at 0.55. Afterwards, the ballast bed with the thickness at 0.35 m was filled in the geometry until reaching the porosity of 0.36. Then, the sleepers (mono-block or nailed sleeper) were placed on the ballast bed. Finally, the crib and shoulder ballast were filled in the geometry until 0.36 porosity. After the model was stabilised, the geometry was deleted, and two new walls were generated to prevent ballast collapse, as shown in Figure 4a.

Note that the sub-ballast layer was not considered in the DEM model, because the studied nailed lengths cannot reach there. In addition, the simulation results were compared between each other. Involving sub-ballast particles in DEM model considerably increases computation costs, due to sub-ballast particles are much smaller than ballast particles.

2.2.4. Simulation conditions

As shown in Table 5, four conditions were simulated, considering different sleeper type (mono-block or nailed sleepers) together with nail number and length. Considering that sleepers with 400 mm length nails can possibly into the subgrade, therefore, conditions of nail length at 100 or 200 mm were simulated to

compare with the experimental tests for model validation. Afterwards, conditions of four nails with length at 100 or 200 mm were simulated, and the results were compared with the former simulation results.

Table 5 Lateral and longitudinal single sleeper push test simulation conditions

Conditions	Sleeper type	Nail number	Nail length (mm)
1	Mono-block	-	-
2	Nailed sleeper	2	100
3	Nailed sleeper	4	100
4	Nailed sleeper	2	200
5	Nailed sleeper	4	200

3. Results and discussions

3.1. Experimental test results and discussions

3.1.1. Lateral and longitudinal resistance

As shown in Figure 6, it presents the relationship between lateral resistance (or longitudinal resistance) and sleeper displacement. The two SSPT conditions are mono-block sleeper (Condition A; Table 2) and nailed sleeper with nail length at 400 mm and shoulder width at 500 mm (Condition B; Table 2).

From the Figure 6a, it can be seen that the lateral resistance of both two sleepers (mono-block or nailed) increase along with the sleeper displacement, and the resistance increment speed reduces as the displacement reaches 1.5 mm. When the displacement exceeds 4 mm, the lateral resistance is stable. The lateral resistance of nailed sleeper is higher than that of mono-block sleeper after 0.5 mm displacements, which means the nails start to resist the sleeper. In most lateral SSPTs, the resistance of 2 mm displacement is counted as the resistance value. At 2 mm displacement, the nailed sleeper has higher lateral resistance value than mono-block sleeper by 53.7%. This means applying the nail sleeper can effectively increase the lateral resistance.

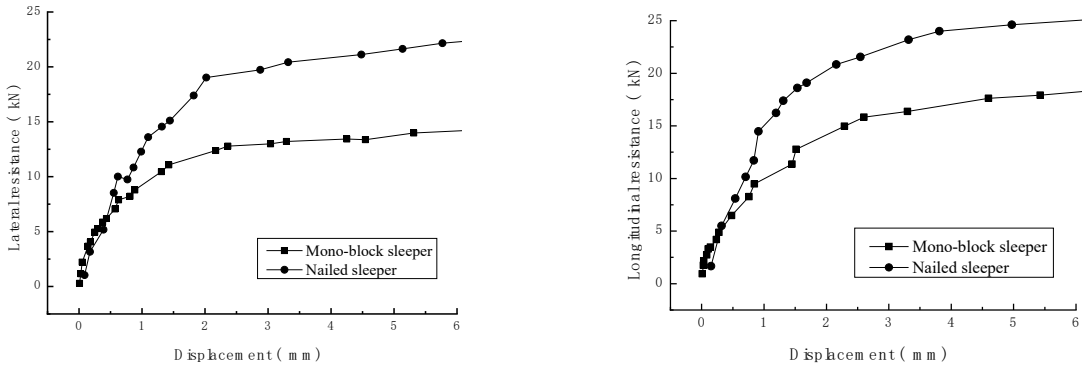

Figure 6 Lateral and longitudinal resistance vs displacement curves (a) Lateral resistance vs sleeper displacement (b) Longitudinal resistance vs sleeper displacement

From Figure 6b, it can be observed that the longitudinal resistance of mono-block and nailed sleepers increase along with the sleeper displacement, and the resistance increment speed slow down when the displacement exceeds 2 mm. As the sleeper displacement is over 4 mm, the lateral resistance becomes stable. The longitudinal resistance of nailed sleeper is higher than that of mono-block sleeper after 0.5 mm displacements, which means the nails start to resist the sleeper. At 2 mm displacement, the nailed sleeper has higher lateral resistance value than mono-block sleeper by 39.2%. This means applying the nail sleeper can effectively increase the longitudinal resistance.

3.1.2. Contribution of lateral and longitudinal resistance

As introduced in Figure 3, lateral (or longitudinal) resistance is made of three parts, ballast bed force, shoulder force and crib force. Comparing the resistance provided by the ballast bed force can confirm how much the nails can increase the resistance, further keeping the track stable. As shown in Table 6, it presents the resistance contribution of nailed sleeper (nail length 400 mm, shoulder width 300 mm) and mono-block

sleeper (shoulder width 300 mm). The ballast bed force of nailed sleeper can occupy the total resistance at 62% (longitudinal resistance) and 46% (lateral resistance), respectively, which are much higher than mono-block sleeper at 54% (longitudinal resistance) and 20% (lateral resistance). This means by installing the nails, the sleeper can be more stable with less influences from the crib or shoulder forces, in other words, at some special areas where small ballast layer profiles were applied, the nail sleeper can be used as a solution to improve track stability.

Table 6 Lateral (or longitudinal) resistance contribution of three parts, ballast bed, shoulder and crib

Contribution	Nailed sleeper		Mono-block sleeper	
	Lateral resistance (kN)	Percentage	Lateral resistance (kN)	Percentage
Ballast bed	10.24	**62%**	4.49	**54%**
Shoulder	3.96	24%	1.24	31%
Crib	2.31	14%	2.58	15%
Total	16.51	100%	8.31	100%
Contribution	Longitudinal resistance (kN)	Percentage	Longitudinal resistance (kN)	Percentage
Ballast bed	8.62	**46%**	2.6	**20%**
Shoulder	1.12	6%	1.06	8%
Crib	8.99	48%	9.54	72%
Total	18.73	100%	13.2	100%

3.1.3. Nail length

The nail length has considerable influences on the lateral resistance, as shown in Figure 7a. From the figure, it can be seen that installing nail can increase the peak value of lateral resistance, and longer nail can increase the lateral resistance. At the sleeper displacement of 2 mm, the lateral resistance increase by 0.83 kN, 6.1% (100 mm nail length), 2.37 kN, 19.1% (200 mm nail length) and 6.65 kN, 53.7% (400 mm nail length).

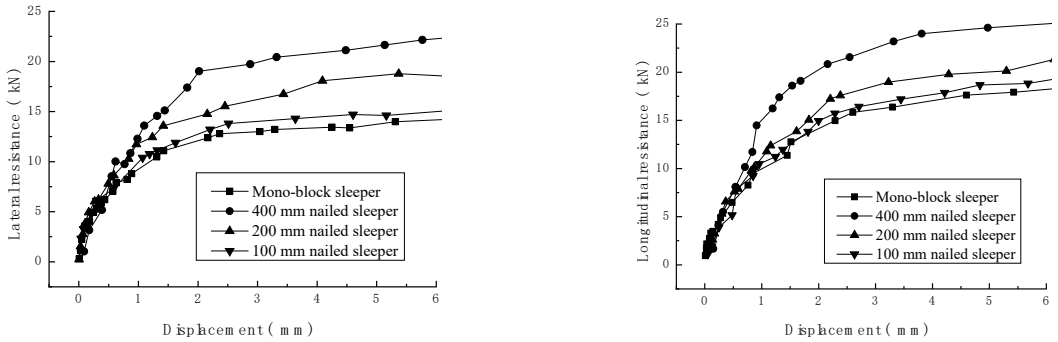

Figure 7 Influence of nail length on lateral and longitudinal resistance (a) Lateral resistance of different nail lengths (b) Longitudinal resistance of different nail lengths

The nail length has also big influences on the longitudinal resistance, as shown in Figure 7b. From the figure, it can be observed that applying nail can increase the peak value of longitudinal resistance, and longer nail can provide higher longitudinal resistance. At the sleeper displacement of 2 mm, the longitudinal resistance increases by 0.77 kN, 5.1% (100 mm nail length), 2.27 kN, 15.2% (200 mm nail length) and 5.87 kN, 39.2% (400 mm nail length).

From the results and discussions, it can be seen using longer nail can improve higher lateral and longitudinal resistance. However, considering that the nail length also influences the drainage problem, specifically, when installing the nail in the subgrade layer, the rainfall can go into the subgrade directly through the nail causing low subgrade capacity. Towards this, in the DEM models, increasing nail numbers are mainly considered to improve lateral and longitudinal resistance.

Note that in the operating railway lines, the ballast layer thickness sometimes is much lower than expected due to the ballast motions towards the lateral direction. In addition, in practise, during the track construction, the ballast layer in most cases cannot reach the required thickness (sometimes no sub-ballast). Therefore, the maximum 200 mm nail length is chosen for the DEM simulations, which is meaningful for real engineering conditions.

3.1.4. Shoulder width

To further study when reducing the ballast profile whether using nailed sleeper can provide enough resistance, the lateral and longitudinal resistance of nailed sleeper at different shoulder widths (300, 400 or 500 mm) are presented in Figure 8. From the figure, shoulder width influences not only the lateral resistance, but also the longitudinal resistance. Wider shoulder width leads to higher resistance.

Specifically, for the lateral resistance (Figure 8a), the nailed sleeper with shoulder width at 300 mm has higher resistance than the mono-block sleeper by 25%, which means it is possible to apply the nailed sleeper to some special areas with less ballast shoulder width (bridge, tunnel). For the longitudinal resistance (Figure 8b), at 2 mm sleeper displacement, when reducing the shoulder width from 500 to 300 mm, the longitudinal resistance reduces by 2.1 kN, 11.2%. Nevertheless, the longitudinal resistance is still 3.77 kN (25.2%) higher than the mono-block sleeper (with 500 mm shoulder width).

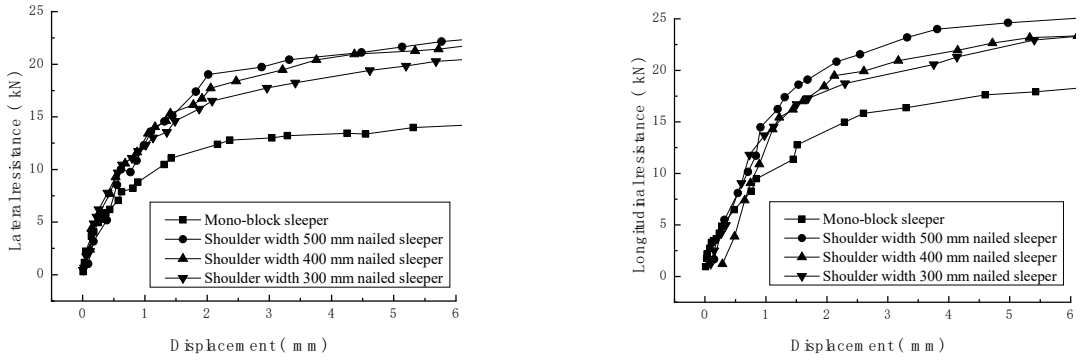

Figure 8 Influences of shoulder width on lateral and longitudinal resistance (a) Influences of shoulder width on lateral resistance (b) Influence of shoulder width on longitudinal resistance

3.2. Numerical simulation results and discussions

3.2.1. Lateral and longitudinal resistance

Considering that when the sleeper displacement exceeds 2 mm in the experimental tests, the increment of the resistance slows down and the resistance almost reaches the peak, therefore, the displacement in the numerical simulations stops at 2 mm. This can sufficiently predict and compare the resistance results and save the computational costs.

As shown in Figure 9, the SSPT models were firstly validated by comparing the numerical results with the experimental results. Afterwards, nailed sleepers with four nails and length at 100 or 200 mm were simulated and their results of resistance were compared with the nailed sleeper with two nails.

From Figure 9a, it can be seen that lateral resistance results of numerical and experimental can be mostly matched, which means the SSPT models can be used for further lateral resistance prediction. From Figure 9b, although there exist a few differences between the experimental results and the numerical results, it is acceptable for further study. Because the longitudinal peak values of the numerical results are 15.70 and 18.06 kN (100 mm length, 200 mm length), which are approximate to the experimental results, i.e. 15.73 and 17.23 kN. The differences are within 4.5%, which is acceptable for further study. In addition, the differences are possibly due to the experimental results of the three kinds of sleepers are close. The close resistance results are possibly due to the nail and the sleeper are not stably locked. In addition, there is a slight rotation when pushing the sleeper longitudinally (more possible to happen than laterally), which causes low resistance in spite of the same sleeper displacement. While in the models the sleeper and nail are completely locked, and the sleeper moves without any rotations.

From Figure 9 c/d, it can be seen that increasing nail number can improve the lateral and longitudinal resistance. When applying the four nails with length at 100 or 200 mm, the peak lateral resistance values

are 16.02 or 20.28 kN, respectively, which are higher than mono-block sleeper (12.78 kN) by 20.2% or 37.0%. while, the peak longitudinal resistance values are 16.17 or 21.73 kN, respectively, which are higher than mono-block by 10.6% or 33.5%. In addition, increasing the nail number improves the lateral resistance by higher percentage than the longitudinal resistance, e.g. 20.2% to 10.6% (4 nails, 100 mm). This is possibly due to the nails can improve the same resistance values at both lateral and longitudinal directions, however, total longitudinal resistance to the sleeper is a higher than total lateral resistance. For this, the increased lateral resistance (4 nails) occupies a lower percentage than the increased longitudinal resistance.

It can be concluded that increasing the nail number can increase the lateral and longitudinal resistance, and the reason is the nails provide more resistance. Thus, for better design this kind of sleeper, it needs to know how the nails interact with ballast particles, which can be presented by contact forces.

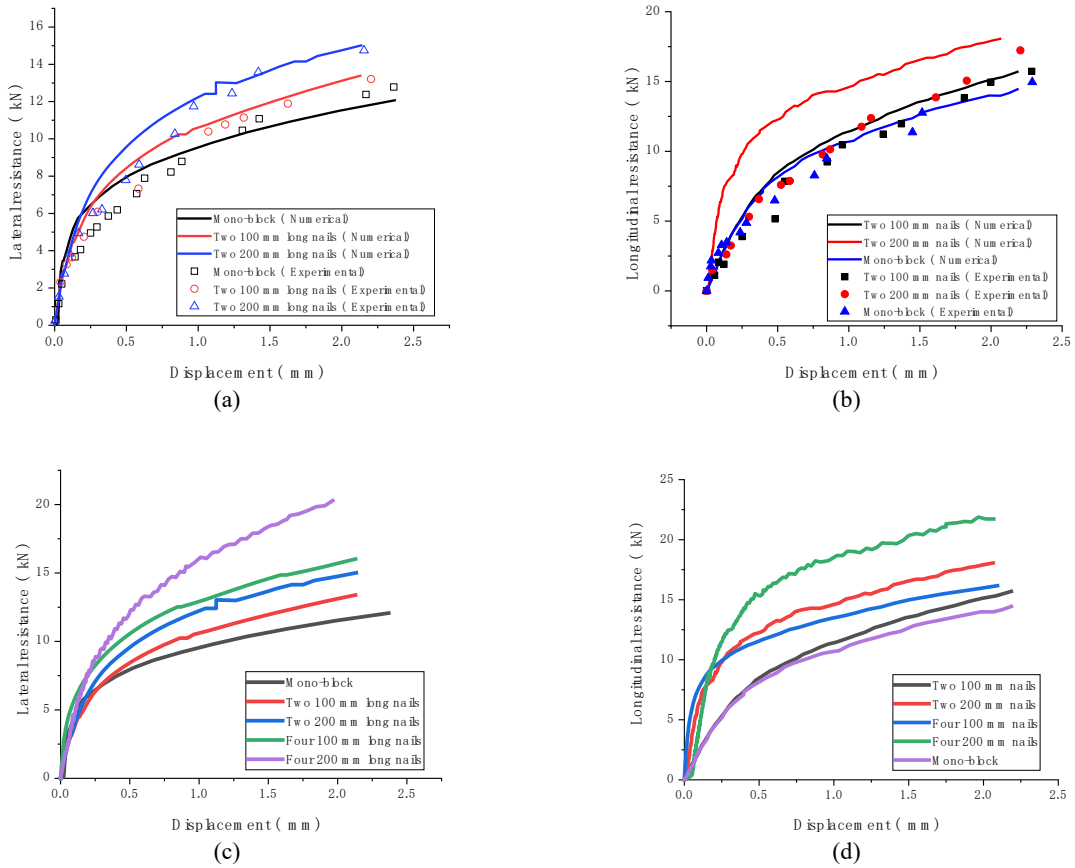

Figure 9 Numerical results of lateral and longitudinal resistance (a) Lateral resistance comparison of numerical and experimental results (b) Longitudinal resistance comparison of numerical and experimental results (c) Numerical lateral resistance results of different nail numbers (d) Numerical longitudinal resistance results of different nail numbers

3.2.2. Contact forces

Figure 10 summarises the contact forces of lateral SSPTs between sleeper and ballast particles at 2 mm sleeper displacement. From Figure 10a, it can be seen that the big contact forces (red lines) appear at shoulder ballast, while differently, the almost all the big contact forces appear at the ballast bed (Figure 10 b/c/d/e). This means the nails help a lot at improving the interaction between sleeper and ballast. Increasing the nail length can improve the ballast particles that contribute to the lateral resistance. From Figure 10e, it can be seen that all the ballast particles that are under the sleeper at the right side of nails take part in providing lateral resistance.

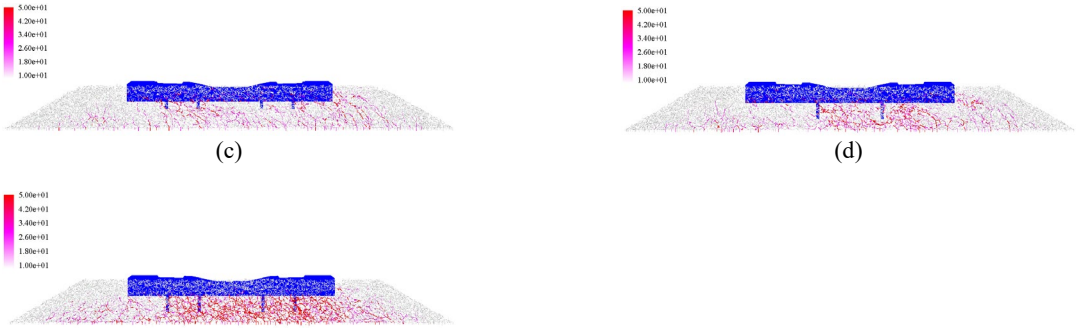

(c) (d)

(e)

Figure 10 Contact forces between ballast particles and sleepers of lateral SSPTs (Legend unit: N) (a) Mono-block sleeper (b) Two nails with length at 100 mm (c) Four nails with length at 100 mm (d) Two nails with length at 200 mm (e) Four nails with length at 200 mm

Figure 11 summarises the contact forces of longitudinal SSPTs between sleeper and ballast particles at 2 mm sleeper displacement. From Figure 11a, it can be seen that the big contact forces (red lines) appear at ballast crib. In addition, as shown in Figure 11b, when the two nails are 100 mm, the contact forces between nails and ballast particles are not obvious (no red lines). However, as shown in Figure 11 c/d/e, increasing nail length (200 mm) or number (4 nails) can make the contact forces (between nail and ballast particles) more obvious, which means more ballast particles take part in providing longitudinal resistance. This proves that although nail sleeper (with nail length at 100 mm) can increase the longitudinal resistance, its effects are not as good as longer nails (or more nails). In other words, applying over 100 mm long nails is recommended in the engineering practise.

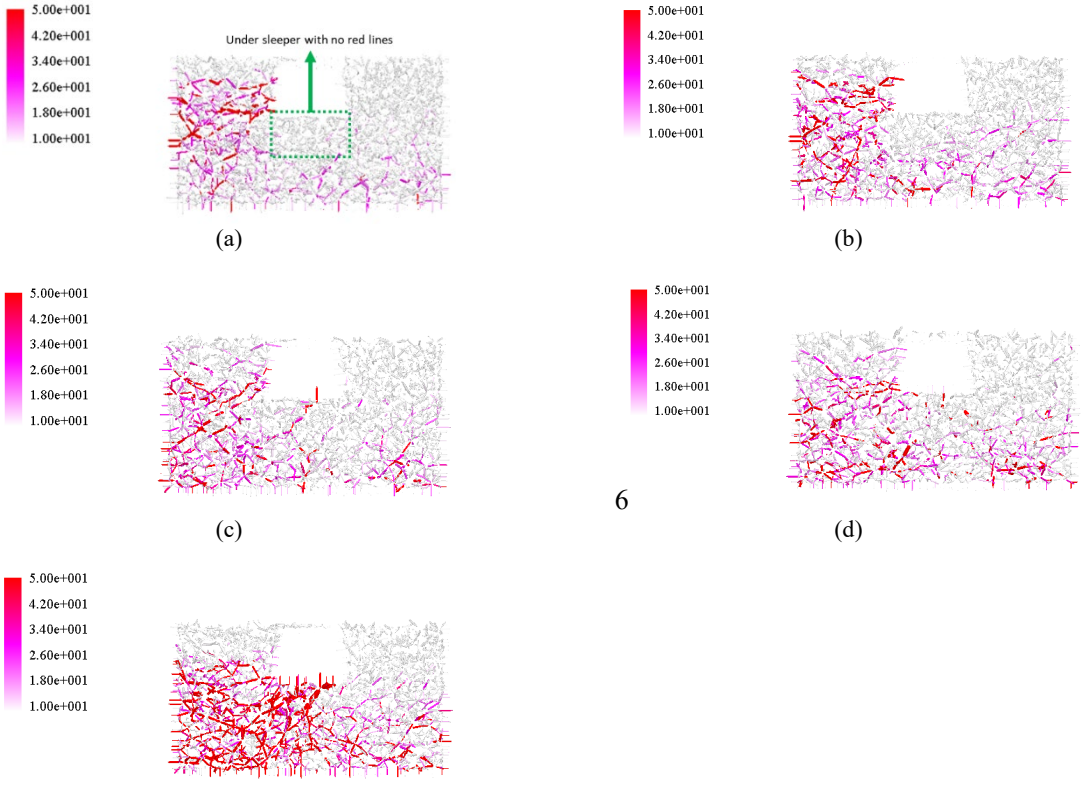

(a) (b)

(c) (d)

(e)

Figure 11 Contact forces between ballast particles and sleepers of longitudinal SSPTs (Legend unit: N) (a) Mono-block sleeper (b) Two nails with length at 100 mm (c) Four nails with length at 100 mm (d) Two nails with length at 200 mm (e) Four nails with length at 200 mm

4. Conclusions and perspectives

4.1. Conclusions

In this study, nailed sleeper was designed based on Chinese mono-block sleeper, and the factors of applying nail sleeper influencing lateral and longitudinal resistance were studied using numerical simulation and experimental tests. The single sleeper push tests (SSPTs) were performed at lateral and longitudinal directions, and the discrete element method (DEM) models of the SSPTs were built. Combining the SSPTs and DEM models, the factors influencing the resistance were studied, including the nail length and nail number. From the results and discussions, the following conclusions can be drawn.

1. The nail sleeper can provide higher lateral and longitudinal resistance than mono-block sleeper by 53.7% and 39.2% (maximum value), respectively.
2. The nail length has influences on the lateral and longitudinal resistance. Longer nails lead to higher resistance, i.e. 100 mm: 6.1% (lateral) and 5.1% (longitudinal); 400 mm: 53.7% (lateral) and 39.2% (longitudinal). From the simulation results, when nail length is longer than 100 mm, the nailed sleeper can provide sufficiently higher longitudinal resistance.
3. When reducing the shoulder ballast width from 500 to 300 mm, the nail sleeper can still provide sufficient lateral and longitudinal resistance, which mean it can be applied to the tracks in some special areas, such as bridge, tunnels and long steep slope.
4. From the simulation results, it was found the interactions between nails and ballast particles are the main factor influencing resistance improvement. Four nails can provide much higher resistance than two nails.

4.2. Perspectives

In this study, the lateral and longitudinal resistance were studied, however, some factor influencing the resistance can have a further study, such as nail diameter and nail shape. In this study, the cylinder steel stick was used as the nail, and the cylinder diameter can influence the nail-ballast interaction. In addition, the cylinder steel stick can be made into other shapes, e.g. cuboid. Most importantly, before applying the nail sleeper to the track in practise, the cyclic loading performance should also be tested.

Another perspective is the tamping procedure consideration for the nailed sleeper track. The tamping squeezing process has little chances to touch the nail, because the nail diameter is not big. In addition, the stone-blowing seems a better idea for nailed sleeper than tamping.

5. Acknowledgements

The study was supported by the China Scholarship Council.

6. References

[1] Zhai, W. (2020). *Vehicle–track coupled dynamics theory and applications*, Springer Singapore.
[2] Bakhtiary, A., Zakeri, J. A., and Mohammadzadeh, S. (2020). "An opportunistic preventive maintenance policy for tamping scheduling of railway tracks." *International Journal of Rail Transportation*, 1-22.
[3] Kish, A., and Samavedam, G. (2013). "Track buckling prevention: theory, safety concepts, and applications." John A. Volpe National Transportation Systems Center (US).
[4] Indraratna, B., and Ngo, T. (2018). *Ballast railroad design: smart-uow approach*, CRC Press.
[5] Jing, G., and Aela, P. (2019). "Review of the lateral resistance of ballasted tracks." *Proceedings of the Institution of Mechanical Engineers, Part F: Journal of Rail and Rapid Transit*, 095440971986635.
[6] Guo, Y., Markine, V., Zhang, X., Qiang, W., and Jing, G. (2019). "Image analysis for morphology, rheology and degradation study of railway ballast: A review." *Transportation Geotechnics*, 18, 173-211.
[7] China, N. R. A. o. t. P. s. R. o. (2014). "Code for design of high speed railway." *TB 1062-2014*.
[8] Zhang, X., Zhao, C., Zhai, W., Shi, C., and Feng, Y. (2018). "Investigation of track settlement and ballast degradation in the high-speed railway using a full-scale laboratory test." *Proceedings of the Institution of Mechanical Engineers, Part F: Journal of Rail and Rapid Transit*, 233(8), 869-881.
[9] Jing, G., Ding, D., and Liu, X. (2019). "High-speed railway ballast flight mechanism analysis and risk management – A literature review." *Construction and Building Materials*, 223, 629-642.
[10] Qian, Y., Mishra, D., Tutumluer, E., and Kazmee, H. A. (2015). "Characterization of geogrid reinforced ballast behavior at different levels of degradation through triaxial shear strength test and discrete element modeling." *Geotextiles and Geomembranes*, 43(5), 393-402.

[11] Gundavaram, D., and Hussaini, S. K. K. (2019). "Polyurethane-based stabilization of railroad ballast–a critical review." *International Journal of Rail Transportation*, 7(3), 219-240.
[12] Kaewunruen, S., Remennikov, A., and Aikawa, A. "Effectiveness of soft baseplates and fastenings to mitigate track dynamic settlement at transition zone at railway bridge approaches." *Proc., Proceedings of the Third International Conference on Railway Technology: Research, Development and Maintenance, Civil-Comp Press*.
[13] Qi, Y., Indraratna, B., Heitor, A., and Vinod, J. S. (2018). "Effect of Rubber Crumbs on the Cyclic Behavior of Steel Furnace Slag and Coal Wash Mixtures." *Journal of Geotechnical and Geoenvironmental Engineering*, 144(2).
[14] Fathali, M., Nejad, F. M., and Esmaeili, M. (2017). "Influence of Tire-Derived Aggregates on the Properties of Railway Ballast Material." *Journal of Materials in Civil Engineering*, 29(1), 04016177.
[15] Sol-Sánchez, M., Moreno-Navarro, F., Rubio-Gámez, M., Manzo, N., and Fontseré, V. (2018). "Full-scale study of Neoballast section for its application in railway tracks: optimization of track design." *Materials and Structures*, 51(2), 43.
[16] Navaratnarajah, S. K., Indraratna, B., and Ngo, N. T. (2018). "Influence of Under Sleeper Pads on Ballast Behavior Under Cyclic Loading: Experimental and Numerical Studies." *Journal of Geotechnical and Geoenvironmental Engineering*, 144(9), 04018068.
[17] Lima, A. d. O., Dersch, M. S., Qian, Y., Tutumluer, E., and Edwards, J. R. (2018). "Laboratory fatigue performance of under-ballast mats under varying loads and support conditions." *Proceedings of the Institution of Mechanical Engineers, Part F: Journal of Rail and Rapid Transit*, 0954409718795920.
[18] Indraratna, B., Hussaini, S. K. K., and Vinod, J. (2013). "The lateral displacement response of geogrid-reinforced ballast under cyclic loading." *Geotextiles and Geomembranes*, 39, 20-29.
[19] Jing, G., Zhang, X., and Jia, W. (2019). "Lateral resistance of polyurethane-reinforced ballast with the application of new bonding schemes: Laboratory tests and discrete element simulations." *Construction and Building Materials*, 221, 627-636.
[20] Esmaeili, M., Nouri, R., and Yousefian, K. (2016). "Experimental comparison of the lateral resistance of tracks with steel slag ballast and limestone ballast materials." *Proceedings of the Institution of Mechanical Engineers, Part F: Journal of Rail and Rapid Transit*, 231(2), 175-184.
[21] Powrie, W., and Le Pen, L. M. (2011). "Contribution of base, crib, and shoulder ballast to the lateral sliding resistance of railway track: a geotechnical perspective." *Proceedings of the Institution of Mechanical Engineers, Part F: Journal of Rail and Rapid Transit*, 225(2), 113-128.
[22] Jing, G., Ji, Y., and Aela, P. (2020). "Experimental and numerical analysis of anchor-reinforced sleepers lateral resistance on ballasted track." *Construction and Building Materials*, 264.
[23] Koike, Y., Nakamura, T., Hayano, K., and Momoya, Y. (2014). "Numerical method for evaluating the lateral resistance of sleepers in ballasted tracks." *Soils and Foundations*, 54(3), 502-514.
[24] Esmaeili, M., Khodaverdian, A., Neyestanaki, H. K., and Nazari, S. (2016). "Investigating the effect of nailed sleepers on increasing the lateral resistance of ballasted track." *Computers and Geotechnics*, 71, 1-11.
[25] Liu, H., Xiao, J., Wang, P., Liu, G., Gao, M., and Li, S. (2018). "Experimental investigation of the characteristics of a granular ballast bed under cyclic longitudinal loading." *Construction and Building Materials*, 163, 214-224.
[26] Zeng, Z., Song, S., Wang, W., Yan, H., Wang, G., and Xiao, B. (2018). "Ballast bed resistance characteristics based on discrete-element modeling." *Advances in Mechanical Engineering*, 10(6), 1687814018781461.
[27] Mohammadzadeh, S., Esmaeili, M., and Khatibi, F. (2018). "A new field investigation on the lateral and longitudinal resistance of ballasted track." *Proceedings of the Institution of Mechanical Engineers, Part F: Journal of Rail and Rapid Transit*, 095440971876419.
[28] Esmaeili, M., Zakeri, J. A., and Babaei, M. (2017). "Laboratory and field investigation of the effect of geogrid-reinforced ballast on railway track lateral resistance." *Geotextiles and Geomembranes*, 45(2), 23-33.
[29] Le Pen, L., Bhandari, A. R., and Powrie, W. (2014). "Sleeper End Resistance of Ballasted Railway Tracks." *Journal of Geotechnical and Geoenvironmental Engineering*, 140(5), 04014004.
[30] De Iorio, A., Grasso, M., Penta, F., Pucillo, G. P., Rossi, S., and Testa, M. (2016). "On the ballast–sleeper interaction in the longitudinal and lateral directions." *Proceedings of the Institution of Mechanical Engineers, Part F: Journal of Rail and Rapid Transit*, 232(2), 620-631.
[31] Khatibi, F., Esmaeili, M., and Mohammadzadeh, S. (2017). "DEM analysis of railway track lateral resistance." *Soils and Foundations*, 57(4), 587-602.
[32] Xiao, J., Zhang, D., Wei, K., and Luo, Z. (2017). "Shakedown behaviors of railway ballast under cyclic loading." *Construction and Building Materials*, 155, 1206-1214.
[33] Guo, Y., Zhao, C., Markine, V., Shi, C., Jing, G., and Zhai, W. (2020). "Discrete element modelling of railway ballast performance considering particle shape and rolling resistance." *Railway Engineering Science*, 28(4), 382-407.
[34] Guo, Y., Zhao, C., Markine, V., Jing, G., and Zhai, W. (2020). "Calibration for discrete element modelling of railway ballast: A review." *Transportation Geotechnics*, 23, 100341.
[35] Guo, Y., Fu, H., Qian, Y., Markine, V., and Jing, G. (2020). "Effect of sleeper bottom texture on lateral resistance with discrete element modelling." *Construction and Building Materials*, 250.
[36] British Standards Institution, B. s. p. B. E. (2013). "Aggregates for railway ballast." British Standards Institution London.
[37] Irazábal, J., Salazar, F., and Oñate, E. (2017). "Numerical modelling of granular materials with spherical discrete particles and the bounded rolling friction model. Application to railway ballast." *Computers and Geotechnics*, 85, 220-229.
[38] Suiker, A. S. J., and Fleck, N. A. (2004). "Frictional Collapse of Granular Assemblies." *Journal of Applied Mechanics*, 71(3), 350.
[39] Esveld, C., and Esveld, C. (2001). *Modern railway track*, MRT-productions Zaltbommel, The Netherlands.